doi.org/10.36721/PJPS.2020.33.5.SP.2393-2398.1

Pharmacokinetics-based analysis of indomethacin's anti-tumor effect and drug efficacy

Zhang Yan[1], Zhang Jun[2], Zhao Zhu[3], Gao Jingjing[3] and Li Ke[4*]

[1]Department of Internal Medicine, The People's Hospital of Huaiyin Jinan, Shandong, China
[2]Medical Section, The People's Hospital of Huaiyin Jinan, Shandong, China
[3]Health ward, The People's Hospital of Huaiyin Jinan, Shandong, China
[4]Shandong Cancer Hospital and Institute, Shandong First Medical University and Shandong Academy of Medical Sciences, Jinan, China

Abstract: Non-steroidal anti-inflammatory drugs are commonly used anti-inflammatory analgesics in clinic. Indomethacin is a kind of NSAIDs and has anti-tumor effect. It can significantly change the growth cycle of cancer cells, inhibit their proliferation. In this paper, the antineoplastic effect of indomethacin and its pharmacokinetic effect were analysed. The result showed that indomethacin had more metabolic distribution in tumor tissues and reached its peak at 4 hours, after that, the clearance rate was slower than that in the blood, with the clearance rate slowest at 6-12 hours. At the same time, the expression of Bcl-2 protein in cancer cells was significantly reduced and weakened, while the expression of Bax protein did not change significantly. Pharmacodynamic studies have proved that IN (Indomethacin) has a strong anti-tumor effect. It can enter into tumor cells through cell membrane and nuclear membrane to have an anti-tumor effect.

Keywords: Pharmacokinetics, tumor-bearing mice, indomethacin, anti-tumor effect.

INTRODUCTION

Indomethacin is a non-steroidal anti-inflammatory drug that has been used for a long time in clinical practice (Hasan *et al.,*2018). It has been reported in the literature that the indole-labeled indomethacin (3H-IN) is introduced into tumor-bearing mice and has a strong tumor affinity (Jalili *et al.,* 2014). In order to further study the metabolic distribution of indomethacin in the tumor and its accumulation in the tumor, and provide a theoretical basis for its further clinical application, this work intends to introduce the indole-labeled indomethacin into the Lewis lung cancer (Emir *et al.,* 2014). The literature on the pharmacokinetics of indomethacin in human plasma and animal plasma and tissues and the anti-tumor mechanism of indomethacin has been reported at home and abroad, but on the plasma and tumor of indomethacin in tumor-bearing mice (Iqbal *et al.,* 2013). The pharmacokinetics in vivo and the main components accumulated in tumor tissues have not been reported at home and abroad. The method of previous research is single, although the radionuclide tracer technology has the advantage of high sensitivity, but it can only measure nuclear radiation, but can not detect the tracer substance of the specified chemical structure (Jana *et al.,* 2010). The high performance liquid chromatography technology makes up for it. Insufficient for this, it can determine the concentration of the drug of the specified chemical structure by the necessary separation and preparation. This study intends to use liquid scintillation measurement (LSC) and high performance liquid chromatography (HPLC) analysis techniques to study the distribution and pharmacokinetics of indomethacin in the blood and tumor of tumor-bearing mice, and its tumor tissue (Kanatt *et al.,* 2007).

Human drug discovery has gone through a new era of discovering drugs from nature, randomly screening for drugs, and discovering and developing new drugs based on mechanisms of action and target structures(Kim *et al.,*2008). With the development of modern biology and molecular genetics, drug research has also entered the 21st century gene-based drug discovery and development period. Molecular nuclear medicine technology is the most basic and important means of molecular biology (Block *et al.,* 2017). It provides us with information about the existence, expression, distribution, and composition of normal and abnormal molecules, making genetic drug discovery and development faster and more convenient (Kolawole *et al.,* 2015). Although the radioisotope tracer technology has the shortcomings of radiation biological effects, its sensitivity is extremely high, so it is still widely used in the pharmacokinetic study of drugs, especially genetic engineering drugs (Lee *et al.,* 2017).

Nuclear instruments can only measure the corresponding ray and cannot detect the tracer of the specified chemical structure (Lazarevic *et al.,* 2017). The HPLC technology that emerged in the late 1960s is another major and leaping innovation in the development of chromatographic technology. Its application in pharmacokinetics, drug treatment research and therapeutic drug monitoring is particularly striking, and it can determine the drug concentration of a given chemical structure substance by the necessary separation and preparation (Lv *et al.,* 2018). Vree TB *et al*. reported the

**Corresponding author:* e-mail: drlikeheadneck@163.com

direct gradient HPLC analysis of indomethacin and its generation in plasma and urine. The product and the product after glucuronidation (Li *et al.,* 2017). There have been a lot of reports on the pharmacokinetics of indomethacin in human plasma and animal plasma and tissues and the anti-tumor mechanism of indomethacin. Studies on the main components of kinetics and anti-tumor effects have not been reported at home and abroad.

MATERIALS AND METHODS

(1) Main instrument: LS580/automatic liquid scintillation meter: produced by Beckmen, USA; LC-10AT high performance liquid chromatograph with SPD-10A visible UV detector and C-R6A data processor: product of Shimadzu Corporation, Japan; SC1100 universal chromatography workstation; XW-80A type vortex mixer: Shanghai Jingke Industrial Co., Ltd.; LD4-2A centrifuge: Shanghai Medical Analytical Instrument Factory; TG332A type micro analytical balance: Shanghai Tianping Instrument Factory.

(2) Main materials and reagents: Indomethacin: chemical purity 100%, medium; 3H-IN: radiochemical purity > 95%, specific activity > 185 GBq/g, labeled by the Institute of Isotopes, China Institute of Atomic Energy, mark laboratory; scintillation fluid: 2,5 diphenyloxazole (PPO) (Hong Kong), 1,4-bis[2-(5-phenyloxazole)]-benzene (POPOP) (Germany), naphthalene, AR grade xylene, anhydrous Ethanol and internal standard naproxen sodium; methanol and acetonitrile were chromatographically pure; the rest of the reagents were of analytical grade.

(3) Experimental animals: C57BL/6 inbred male mice: 66 mice, aged 6-8 weeks, weighing 20 2 g, purchased from experimental animals of China Medical University Center, use license number XYXK (Liao) 2003-0019, production license XCXK (Liao) 2003-0013; Dutch Lewis lung cancer model mouse: purchased from Institute of Materia Medica, Chinese Academy of Medical Sciences

Therapeutic method

(1) Preparation of mouse Lewis lung cancer model

The Lewis lung cancer model rats were sacrificed, the tumor was exposed, and 5 g of well-grown tumor tissue was taken, ground with a grinder, and diluted with 15 mL of physiological saline. Tumors were inoculated subcutaneously into the right anterior humerus of C57BL/6 inbred mice with a syringe, each inoculated with 0.2 mL (single cell suspension number 107 / mL). The tumor to be inoculated is used up to a long diameter of 0.8 to 1.0 cm.

(2) Measurement of 3H-IN distribution in plasma and tumor of tumor-bearing mice by liquid scintillation.

After 66 tumor-bearing mice were numbered, they were randomly divided into 11 groups of 6 rats each. Group 1 mice were not treated as a control group, and the other groups were intragastrically administered with 185 kBq (0.2 mL, containing IN 90 μg) 3H-IN. The cells were taken at 0.5, 1, 2, 3, 4, 6, 9, 12, 24, 36, 48 h and the mice were sacrificed. The tumor tissues were taken out, and the surface was floated with physiological saline. The filter paper was blotted and weighed. The weight was homogenized separately and then nitric acid was added for digestion, and then evenly spread on a filter membrane to dry. The collected blood and tumor tissues were sequentially placed in a liquid scintillation bottle to determine the radioactivity count rate, and the percentage of radioactivity uptake per gram of tissue (%. g-1) was calculated.

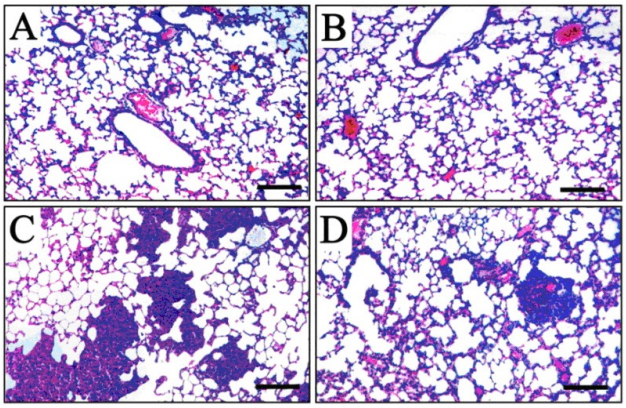

Fig. 1: Effect of IN on the expression of Bcl-2 and Bax proteins in tumor tissues

(3) High performance liquid chromatography analysis

Sample production: Preparation of plasma samples: While carrying out the measurement of the tumor-bearing mouse liquid, collect 1 mL of blood with a heparin-coated conical tube, centrifuge at 3 500r/min for 10min, take the supernatant and set the refrigerator at -20°C. In the test. Preparation of tumor tissue homogenate sample: The previously removed tumor tissue was blotted with filter paper, weighed, placed in a tissue grinder, added to physiological saline at a volume ratio of 1:3, ground into a tissue homogenate, also at 3 500r Centrifuge at /min for 10 min, take the supernatant, and set a refrigerator at 20°C for testing.

Production of indomethacin standard curve: Weigh 25 mg IN with a precision balance, dilute to 25 mL with a volumetric flask to make a 1 g/L stock solution, and dilute with methanol to a concentration of 50, 25, 10, 5, 2.5, 1.25, 0.5 mg/L, a total of 7 A concentration gradient of 50 μL for each concentration was added to 50μL of internal standard (10 mg/L naproxen sodium solution), and 0.1 mL of control group plasma or tumor tissue samples were added. After mixing, 100μ was added. L10% potassium dihydrogen phosphate buffer (pH 2.5), and then add 3 mL of methyl tert-butyl ether, mix well, shake for 20 min,

Table 1: Comparison of body weight, tumor mass and volume between the two groups at the end of the experiment (x ± s)

Group	Number of cases	Rat body weight/g	Tumor mass/g	Tumor volume/ cm^3	Tumor inhibition rate/%	P
Control group	10	24.87± 1.69	7.28± 2.10	7.23± 2.03		< 0.05
Experience group	10	23.36± 0.71	3.28± 1.17	3.25± 1.05	55.05	< 0.05

Table 2: Total Integral Optical Density of Bcl-2 and Bax Protein Positive Expressions in Tumor Tissues of Two Groups (x ± s)

Group	n	Total Integral Optical Density		P
		Bcl-2 Protein	Bax Protein	
Control group	10	100 156± 10 859	85 316± 13 654	< 0.05
Experience group	10	73 817± 8 079	82 857± 13 342	< 0.05
t		6.154	2.101	

Note: P<0.001 compared with the control group; P > 0.05

Table 3: Biodistribution of ^{3}H-IN in tumor and blood of tumor-bearing mice(x ± s, n= 6)

Time/h	Radioactive intake /(%. g^{-1})		P
	Tumor tissue	plasma	
0.5	0.16± 0.27	0.58± 0.26	< 0.05
1.0	0.36± 0.29	0.31± 0.23	> 0.05
2.0	0.38± 0.05	0.45± 0.27	> 0.05
3.0	0.47± 0.26	0.43± 0.09	> 0.05
4.0	0.68± 0.33	0.36± 0.01	> 0.05
6.0	0.39± 0.11	0.18± 0.26	< 0.05
9.0	0.36± 0.06	0.16± 0.22	< 0.05
12.0	0.34± 0.03	0.08± 0.11	< 0.01
24.0	0.13± 0.06	0.06± 0.02	> 0.05
36.0	0.09± 0.02	0.04± 0.12	> 0.05
48.0	0.06± 0.24	0.01± 0.02	> 0.05

centrifuge at 3 500r / min for 10 min, take the supernatant, to 60°C water bath air After drying, the residue was dissolved in 100μL of anhydrous methanol, vortexed for 1 min, and 50μL was taken for high performance liquid chromatography. Taking the IN concentration as the abscissa, the measured peak height ratio of IN to the internal standard naproxen sodium in the plasma or tumor homogenate at each concentration point is the standard curve of indomethacin and linearized.

Determination of drug concentration in plasma and tumor tissue: Take 50μL of anhydrous methanol to supplement the volume of the IN standard solution, add 50μL of internal standard (10mg/L naproxen sodium solution) and then add 0.1 mL of the plasma and tumor tissue sample to be mixed. The remaining methods are the same as above, and the ratio of the peak height of the IN and the internal standard naproxen sodium in the plasma and tumor tissues at each time point is substituted into the regression equation of the standard curve, thereby obtaining the drug concentration at each time point.

Ethical approval

The animal experiment was completed in the animal experiment management center. The whole project was supervised by the experimental animal ethics committee, and passed the ethical review, ethical approval number as 18TPHHJ13.

STATISTICAL ANALYSIS

All the data were processed by SPSS 21.0 statistical software. All measurements were expressed by t-test. The test level was P= 0.01, P<0.05 was significant, P<0.01 was extremely significant. The drug concentration data of plasma and tumors in different phases were processed by the practical pharmacokinetic program DAS ver1.0. A two-compartment model was selected and the weight coefficient was 1/cc to fit the drug-time curve.

RESULTS

Comparison of body weight, tumor mass and volume between the two groups at the end of the experiment

Table 1 shows that the inhibition rate of IN in the experimental group is 55.05%, which indicates that IN can significantly inhibit the growth of Lewis lung cancer. Compared with the control group, the quality of tumors in

Table 4: Indomethacin concentration in tumor and plasma of tumor-bearing mice (x ± s, n= 6)

Time/h	Radioactive intake /(%. g-1)		P
	Tumor tissue	plasma	
0.5	3.10±1.06	11.64±2.70	< 0.05
1.0	3.73±0.26	9.25±4.02	< 0.01
2.0	3.91±2.48	7.38±1.63	< 0.01
3.0	6.08±2.42	7.19±1.69	> 0.05
4.0	9.77±0.85	4.80±1.34	< 0.01
6.0	3.06±2.18	6.26±1.55	< 0.01
9.0	1.72±0.75	4.83±1.56	< 0.01
12.0	1.30±0.10	3.83±1.62	< 0.01
24.0	0.95±0.45	2.36±1.72	> 0.05
36.0	0.89±0.45	0.76±1.87	> 0.05
48.0	0.37±1.25	0.36±1.07	> 0.05

the experimental group was significantly different (t= 3.355, P<0.01), and the volume of tumors was significantly different (t= 5.527, P<0.001).

Effect of IN on the expression of Bcl-2 and Bax protein in tumor tissues

The effect of IN on the expression of Bcl-2 and Bax proteins in tumor tissues is shown in table 2. Bcl-2 and Bax proteins are expressed in all Lewis lung cancers. Bcl-2 and Bax positive cells were mainly located in the cytoplasm. Compared with the control group, the expression of Bcl-2 protein in the experimental group was significantly reduced and weakened. The expression intensity of Bax protein in the experimental group was not significantly different from that in the control group. The total values of Bcl-2 and Bax integral optical densities are listed in table 2. As can be seen from table 2, IN could significantly down-regulate the expression of Bcl-2 protein (t= 6.154, P<0.001), but had no significant effect on the expression of Bax protein (t= 2.101, P>0.05).

Biodistribution of 3H-IN in blood and tissues of tumor-bearing mice

The biodistribution of 3H-IN in the blood and tumor tissues of tumor-bearing mice is shown in table 4. The results in table 1 show that 3H-IN has more metabolic distribution in the tumor tissue, reaching a peak at 4 h. After that, the clearance rate is significantly slower than the blood, and the excretion is the slowest at 6-12 h, and it is 6h after the administration. The percentage of total dose of radioactive drug per gram of tumor tissue was significantly higher than that of blood (P<0.05); at 12 hours, there was a significant difference in the distribution of radioactivity between tumor and blood (P<0.01); tumor and blood The radioactive uptake ratio starts >1 at 3h and gradually increases with time, and reaches the maximum at 12h, which is basically consistent with the results reported in the literature. This indicates that 3H-IN has significant radioactive concentration in the tumor tissue of the tumor-bearing mice and can remain in the tumor tissue for a long time. Pharmacodynamic studies have proved that IN has a strong inhibitory effect on tumors, so IN has long been concentrated in tumor tissues to provide a sufficient basis for its anti-tumor effect.

DISCUSSION

The essence of nuclear medicine is "molecular", which can observe the fate and changes of metabolites, drugs and other molecules in the body and in the normal or morbid state in vivo (Mensor *et al.,* 2001). "Molecular Nuclear Medicine" is the latest development in nuclear medicine and is the most prominent new branch of nuclear medicine in contemporary times (McIlwain *et al.,* 2013). Its development relies mainly on the development and advancement of modern molecular biology techniques, tracer techniques and nuclides detection instruments (Luo, 2001). In recent years, the birth of molecular biology has injected unprecedented vitality into life sciences (Marmitt *et al.,* 2018; Wilbert *et al.,* 2018). Molecular nuclear medicine, which has been developed in combination with nuclear medicine, has the advantage of both parents and opens up a bright space for the research and development of drugs(Nabavi *et al.,* 2016). In recent years, molecular nuclear medicine technology has made great progress in drug research (Pistevou *et al.,* 2015). Such as radionuclide tracer technology in genetic engineering drugs (mainly multi-protein drugs) pharmacokinetic studies and stable nuclides tracing combined with gas chromatography-mass spectrometry (GC-MS) technology in drug metabolism and pharmacokinetics It has been widely used in research. In addition, the application of PET has made nuclear medicine a new era in molecular nuclear medicine(Miloso *et al.,*2008). At present, positron emission tomography (PET) technology is rapidly developing, and its value for drug research and development is receiving more and more attention, and it has broad application prospects (Virginia *et al.,*2018). Broadly speaking, receptors, antibodies, polypeptides, and radiopharmaceuticals are

important research objects in molecular nuclear medicine (Nordberg, 2006). Marking, instrumentation, computer, protection, ultra-micro analysis, autoradiography, PET, etc. are all necessary technical tools for molecular nuclear medicine and an indispensable tool for researching innovative drugs(Sung *et al.,*2017).

The radioisotope tracer technology has high sensitivity and is widely used in drug pharmacokinetics, distribution, metabolism and excretion, such as 1i yun-chun, such as lactosyl human growth hormone labeled with radionuclides 125I and human growth. Hormones The quantitative distribution of these two drugs in mice was studied, and radioactivity in the organs was measured. Wang CH *et al*. used 3H-labeled butylphthalide (3H-NBP) to introduce the urine and feces of different time periods to measure their radioactivity. Liquid scintillation measurement technology has been widely used in the absorption, distribution, excretion, metabolism, radioimmunoassay, receptor determination, structure and function of biomacromolecules, and genetic engineering. Radiolabeling is required for radiolabeled drug-binding chromatography-mass spectrometry for drug metabolism studies(Sheng *et al.,* 2015). In recent years, the stable nuclear labeling technique (SIL) has been successfully used to study the absorption, distribution, biotransformation, excretion, interaction and stereoselectivity of drugs.

In this experiment, ^{3}H-IN was introduced into tumor-bearing mice, and its tumor tropism and pharmacokinetics of IN prodrugs in plasma and tumor of tumor-bearing mice were observed (Rodriguez *et al.,* 2019). More metabolic distribution, and longer residence time, the most excretion at 6-12h (Vekov *et al.,* 2015; Yasmina *et al.,* 2019). At 6h and 9h after administration, the percentage of total dose of radioactive drug per gram of tumor tissue in the tumor-bearing mice was significantly different from blood. ($P<0.05$); the difference between tumor and blood was extremely significant at 12h ($P< 0.01$); the radioactivity ratio of tumor to blood began to >1 at 3h, gradually increased with time, and the maximum value was 12h. It is basically consistent with the results reported in the literature (Sun *et al.,* 2019). It indicated that ^{3}H-IN has obvious radioactive concentration in the tumor tissues of tumor-bearing mice, which proves that ^{3}H-IN has good tumor tissue affinity and can remain in tumor tissues for a long time (Trzeciak *et al.,* 2016). Studies have shown that IN has a strong inhibitory effect on tumors, and long-term drug concentration provides a sufficient basis for its anti-tumor effect (Santarelli *et al.,* 2016).

The results of HPLC showed that the protoplast form of IN reached the peak concentration in the tumor tissue at 4h, and then disappeared rapidly, no accumulation occurred, and the drug concentration in the tumor tissue was lower than the blood concentration in 6-12h. There was a significant difference between the two. The difference ($P<0.01$), compared with the results of radioactivity distribution in ISC-measured tumors, showed that the main part of 3H-IN accumulation in anti-tumor effect at 6-12h was not the prototypic form of IN, probably its phase I (DMI and DBI). Or a phase II (glucuronic acid binding reactant) metabolite or a mixture of several metabolites thereof.

CONCLUSION

In this study, the tumoriphilic effect of tritium labelled indomethacin (3H-IN) was observed by liquid scintillation assay (ISC) and high performance liquid chromatography (HPLC). The pharmacokinetic characteristics of indomethacin in tumor-bearing mice were studied. It was confirmed that indomethacin had a good affinity for tumor tissue and its drug prototype was not anti-tumor. Main ingredients. Indomethacin has a strong affinity to target organs of tumors, selectively concentrated in tumors and prolonged retention time in tumors, which is conducive to the treatment of tumors. With the increase in the number of doses of IN drugs, there is a strong inhibition of tumors and anti-tumor effects, which provide reliable evidence for the anti-tumor mechanism of indomethacin.

REFERENCES

Block T, Petrides G and Kushner H (2017). Mifepristone plasma level and glucocorticoid receptor antagonism associated with response in patients with psychotic depression, *J. Clini. Psycho.*, **37**(5): 505.

Emir S, Sozen S, Bali I, GUrdal SO, Turan BC, Yıldırım O and Yetisyigit T (2014). Outcome analysis of laporoscopic D1 and D2 dissection in patients 70 years and older with gastric cancer. *Int. J. Clin. Exp. Med.,* **7**(10): 3501-3511.

Hasan MK, Friedman TC, Sims C, Lee DL, Espinoza-Derout J and Ume A (2018). α7-Nicotinic acetylcholine receptor agonist ameliorates nicotine plus high-fat diet-induced hepatic steatosis in male mice by inhibiting oxidative stress and stimulating AMPK signaling. *Endocr.,* **159**(2): 931-944.

Iqbal T, Hussain AI, Chatha SAS, Naqvi SAR and Bokhari TH (2013). Antioxidant activity and volatile and phenolic profiles of essential oil and different extracts of wild mint (Mentha longifolia). from the Pakistani Flora. *J Anal Methods Chem,* **13**(2): 53-64.

Jalili C, Salahshoor MR and Naseri A (2014). Protective effect of Urtica dioica L. against nicotine-induced damage on sperm parameters, testosterone and testis tissue in mice. *Iran J. Reprod. Med.*, **12**(7): 401-418.

Jana K, Samanta PK and De Kumar D (2010). Nicotine diminishes testicular gametogenesis, steroidogenesis, and steroidogenic acute regulatory protein expression in adult albino rats: possible influence on pituitary gonadotropins

and alteration of testicular antioxidant status. *Toxicol. Sci.,* **116**(7): 647-659.

Kanatt SR, Chander R and Sharma A (2007). Antioxidant potential of mint (Mentha spicata L.). in radiation-processed lamb meat. *Food Chem.,* **100**(12): 451-458.

Kim HP, Park H, Son KH, Chang HW and Kang SS (2008). Biochemical pharmacology of biflavonoids: Implications for anti-inflammatory action. *Arch Pharm Res.,* **31**(3): 265-273.

Kolawole TA, Oyeyemi WA, Adigwe C, Leko B, Udeh C and Dapper DV (2015). Honey attenuates the detrimental effects of nicotine on testicular functions in nicotine treated wistar rats. *Niger J. Physiol. Sci.,* **30**(5): 11-16.

Lazarevic-Pasti T, Leskovac A, Momic T, Petrovic S and Vasic V (2017). Modulators of acetyl cholinesterase activity: From Alzheimer's disease to anti-cancer drugs. *Curr. Med. Chem.,* **24**(30): 3283-3309.

Lv C, Zhou Y and Wang Y (2018). Emergency Nursing Intervention Procedure for Cerebral Infarction Thrombolysis Patients with Neurological Defects, *Bolet. D. Mala. Y. Sal. Amb.,* **58**(5): 148-153.

Lee JK and Kim NJ (2017). Recent advances in the inhibition of p38 MAPK as a potential strategy for the treatment of Alzheimer's disease. *Molecules* **2**2(8): 1287.

Li S, Sun X, Xu L, Sun R, Ma Z, Deng X, Liu B, Fu Q and Qu R (2017). Baicalin attenuates in vivo and in vitro hyperglycemia-exacerbated ischemia/reperfusion injury by regulating mitochondrial function in a manner dependent on AMPK. *Eur. J. Pharmacol*., **815**(2): 118-126.

Luo Y (2001). *Ginkgo biloba* neuroprotection: Therapeutic implications in Alzheimer's disease. *J. Alzheimers. Dis.,* **3**(4): 401-407.

Marmitt DJ, Bitencourt S, Silva AC, Rempel C and Goettert MI (2018). Medicinal plants used in Brazil public health system with neuroprotective potential: A systematic review. *Bol. Latinoam. Caribe Plant Med. Aromat.,* **17**(2): 84-103.

McIlwain DR, Berger T and Mak TW (2013). Caspase functions in cell death and disease. *Cold Spring Harb Perspect. Biol.,* **5**(4): a008656.

Mensor FS, Menezes CC, Leitao AS, Reis TC, dos Santos CS and Coube SG (2001). Screening of Brazilian plant extracts for antioxidant activity by the use of DPPH free radical method. *Phytother. Res.,* **15**(1): 127-130.

Miloso M, Scuter A, Foudah D and Tredici G (2008). MAPKs as mediators of cell fate determination: An approach to neurodegenerative diseases. *Curr. Med. Chem.,* **15**(6): 538-548.

Nabavi SF, Braidy N, Orhan IE and Nabavi SM (2016). *Rhodiola rosea* L. and Alzheimer's disease: From farm to pharmacy. *Phytother. Res.,* **30**(4): 30-36.

Nordberg A (2006). Mechanisms behind the neuroprotective actions of cholinesterase inhibitors in Alzheimer disease. *Alzheimer Dis. Assoc. Disord.,* **20**(2 Suppl 1): S12-S18.

Pistevou K, Zygogianni A and Kantzou I (2015). Splenic irradiation as palliative treatment for symptomatic splenomegaly due to secondary myelofibrosis: A multi-institutional experience. *J. BUON.,* **20**(4): 1132-1136.

Rodriguez A, Nathalie P and Rivero A (2019). Risk factors for Hepatitis B virus infection, *Bolet. De Mala. Y Salud Ambi.,* **59**(3): 26-30.

Sun Q and Li Q (2019). Observing and Analyzing the Adverse Reactions and Nursing Measures of Gadopentetate in Magnetic Resonance, *Bolet. De Mala. Y Salud Ambi.,* **59**(3): 19-25.

Sung K, Sang-Ho J, Kyoung HP, Hyun-Sook K, Sang-Jin H and Woo JP (2017). Functional recovery of regional myocardial deformation in patients with takotsubo cardiomyopathy. *J. Cardi.,* **70**(1): 68-73.

Sheng W, Zhang B, Chen W, Gu D and Gao W (2015). Laparoscopic colectomy for transverse colon cancer: Comparative analysis of short- and long-term outcomes. *Int. J. Clin. Exp. Med.,* **8**(9): 16029-16035.

Santarelli M, Mascitti R, Galeazzi A, Marziali F (2016). Oral ulcer by *Sphingomonas paucimobilis*: First report. *Intern. J. Oral and Maxi. Sur.,* **45**(10): 1280-1282.

Trzeciak P and Wozakowska-Kapłon B (2016). Comparison of Inhospital and 12- and 36-Month Outcomes After Acute Coronary Syndrome in Men Versus Women <40 Years (from the PL-ACS Registry). *Am. J. Cardiol*., **118**(9): 1300-1305.

Virginia MA, Laura V and Hernandez-Madrigal J (2018). Physical and nutritional characterization of tuber meal of "Malanga" (*Colocasia esculenta* L. Schott) of Actopan, Veracruz, Mexico, *Archi. Latin. D. Nutr.,* **68**(2): 175-183.

Vekov T and Lebanova H (2015). Pharmacotherapeutic recommendations for application of target oncological drug therapies for treatment of breast cancer in Bulgaria - therapeutic efficacy and cost effectiveness. *J. Buon.,* **20**(6): 1420-1425.

Wilbert S, Tatyana A and Shamliyan (2018). Dietary Sodium Interventions to Prevent Hospitalization and Readmission in Adults with Congestive Heart Failure. *The Amer. J. Medi.,* **131**(4): 365-370.

Yasmina N, Rodriguez B and Cohinta H (2019). Improved metabolic control for diabetes mellitus, *Bolet. De Mala. Y Salud Ambi.,* **59**(3): 56-59.